Supporting Information

Fluoranthene-o-Carborane Dyad: Exploring Thermochromism and Mechanochromism in Crystalline Systems

Na Li, Xueyan Wu*, Yan Lv, Jinxia Chi, Jixi Guo*

State Key Laboratory of Chemistry and Utilization of Carbon Based Energy Resources, College of Chemistry, Xinjiang University, 830017 Urumqi, China.

Email: Wuxy90@xju.edu.cn; jxguo1012@163.com

Fax: +86-991-8588883; Tel: +86-991-8583083.

Table S1. Crystallographic data of SOF and DOF

Compounds	SOF	DOF
CCDC	2340882	2323066
Empirical formula	$C_{18}H_{20}B_{10}$	$C_{34}H_{28}B_{10}$
Formula weight	344.44	544.66
Temperature	301.00 K	273.00 K
Crystal system	monoclinic	monoclinic
Space group	Cc	$P2_1/n$
Unit cell dimensions	a = 10.47 Å α= 90.00° b =24.56 Å β= 92.49° c = 7.24 Å γ= 90.00°	a = 19.32 Å α= 90.00° b = 6.63 Å β= 106.80° c = 26.86 Å γ= 90.00°
Volume /Å^3	1859.20	3294.80
Z	4	4
Density (calculated)	1.23 g/cm^3	1.09 g/cm^3
Absorption coefficient	0.06 mm^{-1}	0.42 mm^{-1}
F(000)	712	1128
Crystal size	0.12 × 0.08 × 0.01 mm^3	0.12 × 0.10 × 0.08 mm^3
Index ranges	-13 ⩽ h ⩽ 13, -31 ⩽ k ⩽ 31, -9 ⩽ l ⩽ 9	-20⩽ h ⩽22, -7⩽ k ⩽6, -31⩽ l ⩽32
Reflections collected	22912	21651
Independent reflections	4241 [R(int) = 0.0915]	5760 [R(int) = 0.0708]
Absorption correction	Semi-empirical from equivalents	Semi-empirical from equivalents
Refinement method	Full-matrix least-squares on F^2	Full-matrix least-squares on F^2
Data / restraints / parameters	4241 / 2 / 253	5760 / 0 / 397
Goodness-of-fit on F^2	1.04	1.26
Final R indices [I>2σ (I)]	R_1 = 0.05, wR_2 = 0.13	R_1= 0.09, wR_2 = 0.29
R indices (all data)	R_1 = 0.08, wR_2 = 0.15	R_1= 0.12, wR_2 = 0.31
Largest diff. peak and hole	0.12/-0.18	0.38/-0.41

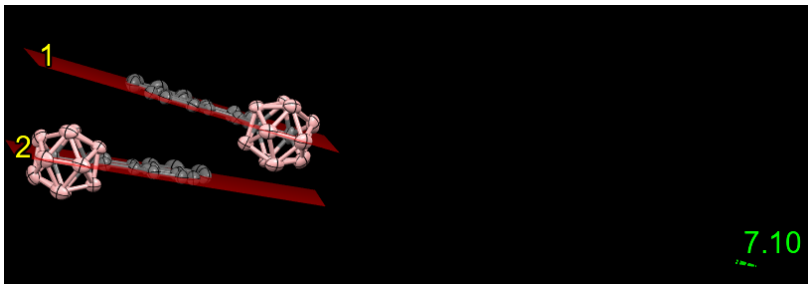

Figure S1. The angle between the two planes of fluoranthene molecule in SOF.

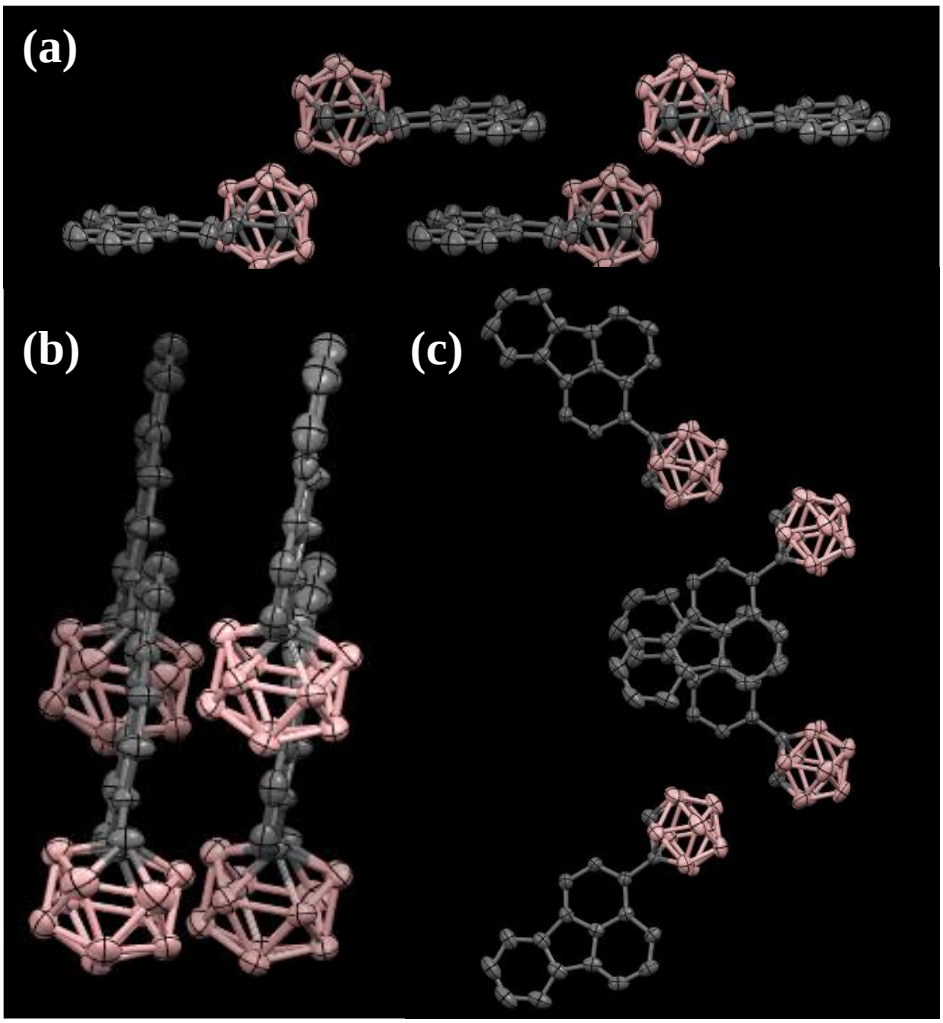

Figure S2. The stacking diagram of SOF in the (a) a, (b) band (c) c axis direction

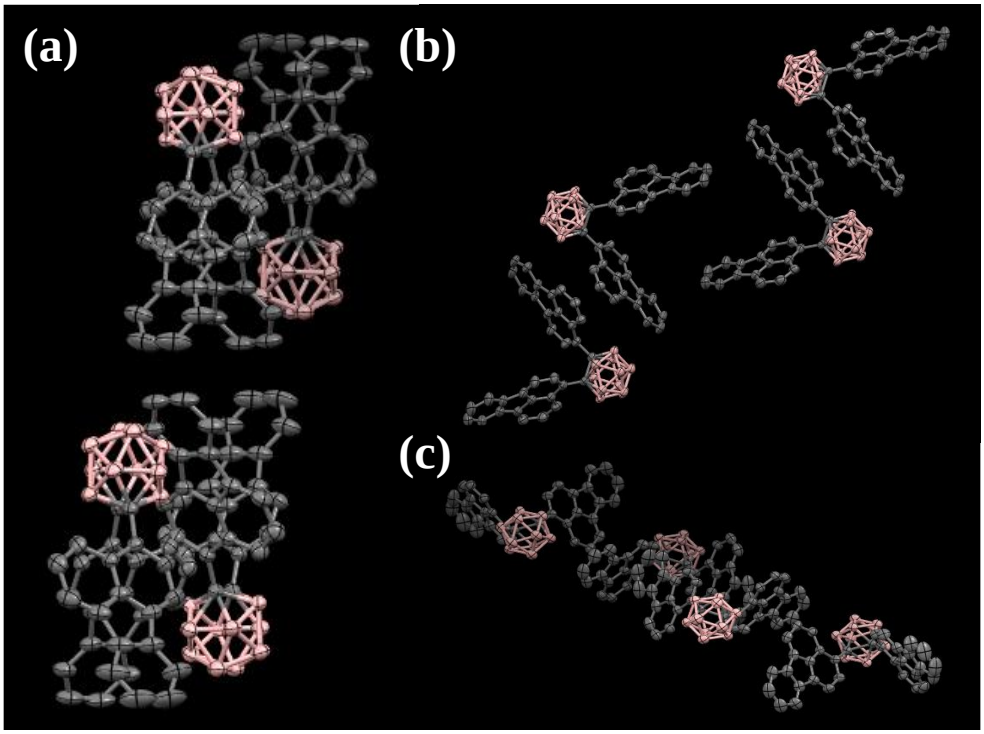

Figure S3. Molecular packing structures of DOF in the (a) a, (b) b and (c) c axis direction

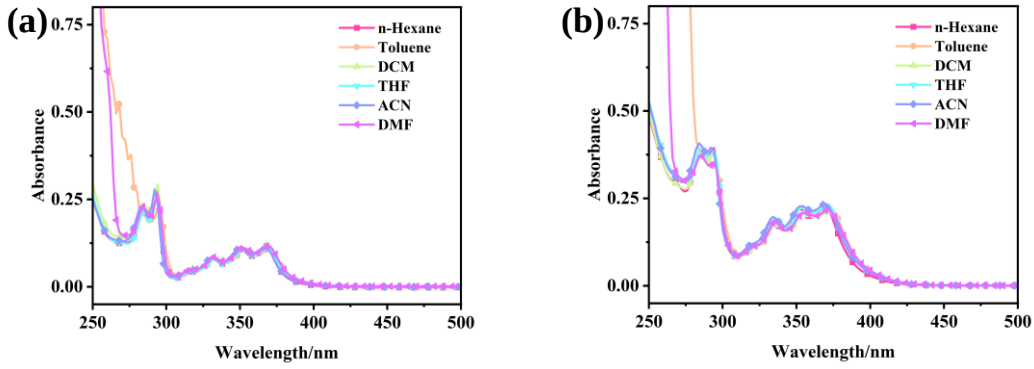

Figure S4. UV-Vis absorption of (a) SOF and (b) DOF in different solvents ($c = 1.0\times10^{-5}$ M, 20 °C).

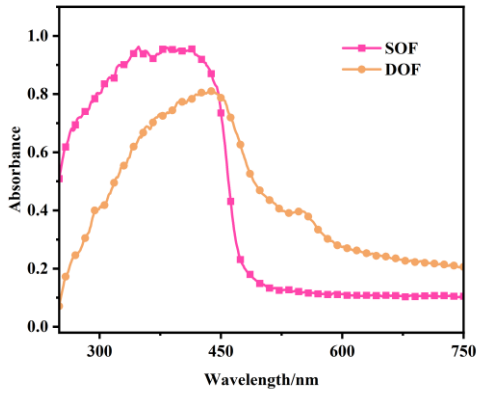

Figure S5. UV-Vis absorption of (a) SOF and (b) DOF in solid state

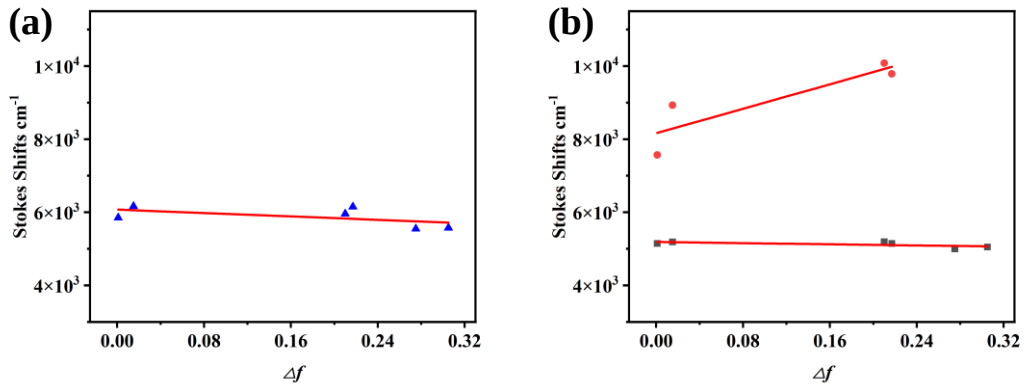

Figure S6. Mataga-Lippert plot of (a) SOF and (b) DOF measured in various solvents.

The simplest consideration for general solvent effect is the Lippert-Mataga equation, by assuming that same excited-state is involved in absorption and emission, and energy difference between the ground- and excited-state is only proportional to solvent orientation polarizability (Δf).

$$\Delta\nu = \frac{2\Delta f}{4\pi\varepsilon_0 hca^3}\left(\mu_e\text{-}\mu_g\right)^2 + \text{constant} \qquad (1)$$

$$\Delta f = \frac{\varepsilon\text{-}1}{2\varepsilon+1} - \frac{n^2\text{-}1}{2n^2+1} \qquad (2)$$

where $\Delta\nu = \nu_{abs} - \nu_{em}$ stands for Stokes' shift, ν_{abs} and ν_{em} are absorption and emission (cm^{-1}), h is the Planck's constant, c is the velocity of light in vacuum, a is the radius of the solvent cavity in which the fluorophore resides (Onsager cavity radius). Δf is the orientation polarizability, μ_e and μ_g is the ground-state dipole in the ground-state geometry and the excited dipole in the excited-state geometry and ε_0 is the permittivity of the vacuum.

Table S2. Absorption and emission spectra of SOF and DOF.[a]

Solvent	SOF			DOF			Δf
	λ_{abs}(nm)	λ_{em}(nm)	Stokes shift(cm^{-1})	λ_{abs}(nm)	λ_{em}(nm)	Stokes shift(cm^{-1})	
***n*-hexane**	368	469	5851	368	454/510	5147/7566	0.001
Toluene	368	476	6165	372	461/557	5189/8928	0.014
DCM	367	474	6150	370	457/580	5145/9785	0.217
THF	369	473	5958	370	458/590	5193/10078	0.210
ACN	368	463	5575	370	455	5049	0.305
DMF	369	464	5548	372	457	4999	0.275

[a]Measured in various solution (1×10^{-5} M) at room temperature, SOF (λ_{ex} = 369 nm), (b) DOF (λ_{ex} = 371 nm), respectively.

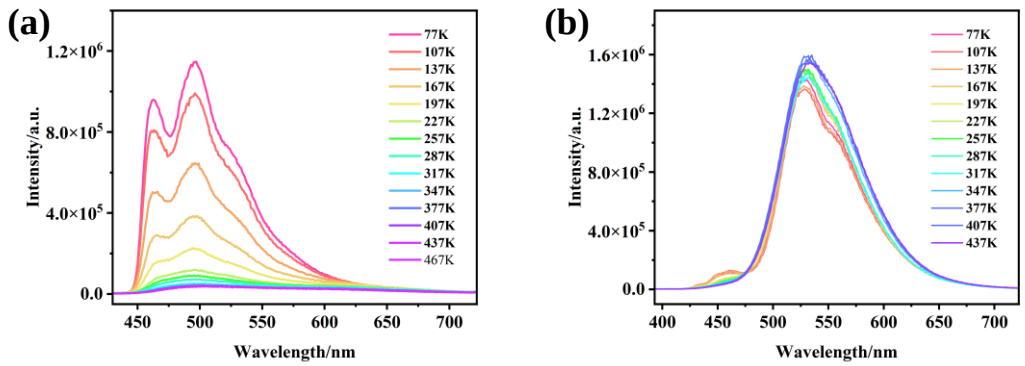

Figure S7. PL spectra of (a) SOF and (b) DOF in the solid state during heating from 77 to 333 K.

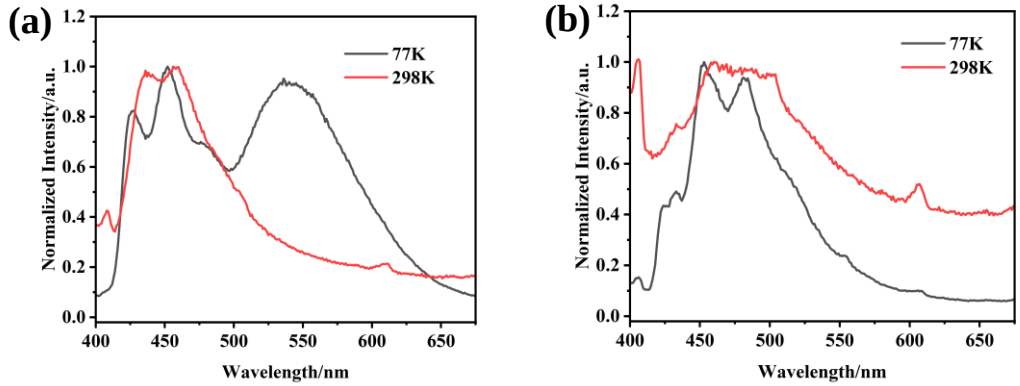

Figure S8. The PL spectra of (a) SOF (λ_{ex} =369 nm) and (b) DOF (λ_{ex} =371 nm) in 2-MeTHF at r. t. (red line) and 77 K (black line), $c = 1.0 \times 10^{-5}$ M.

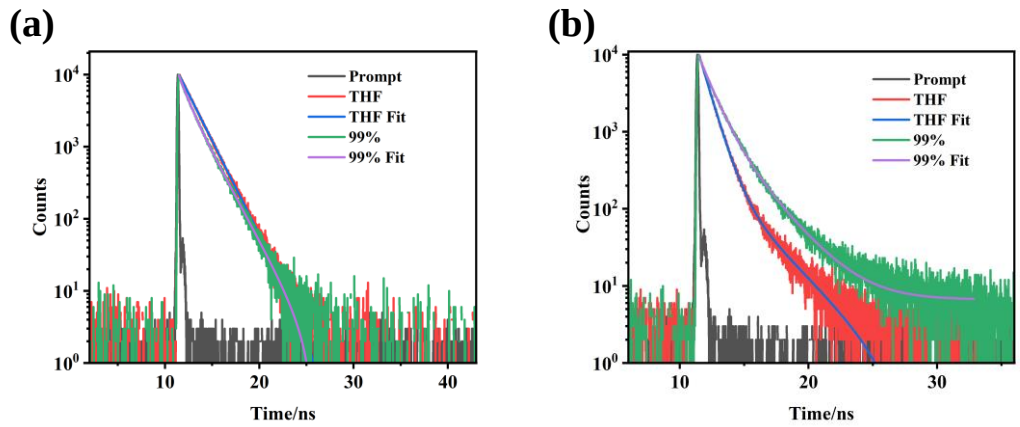

Figure S9. Decay profiles of fluorescence lifetime measurement of (a) SOF and (b) DOF in the mixed solvent of THF/H_2O (1/99) and THF (c=1.0 × 10^{-5} M, λex = 371 nm 25 °C)

Table S3. Photophysical parameters of SOF and DOF in different states

Sample	state	τ_f(ns)[d]	$k_{r(10^7 s^{-1})}$[e]	$k_{nr(10^7 s^{-1})}$[e]
SOF	Sol[a]	16.65	-[f]	-[f]
	Agg[b]	15.62	0.30	6.10
	Solid[c]	33.99/326	0.02	2.90
DOF	Sol[a]	9.83	-[f]	-[f]
	Agg[b]	13.88	0.40	6.70
	Solid[c]	13.78	1.30	5.90

[a] THF, [b] f_w=99%,[c] solid， [d] The excitation wavelength of life test is 371 nm, [e] The radiative transition rate constant k_r and the nonradiative transition rate constant k_r are calculated by the following formula：$k_r=\Phi_f/\tau_f$, $k_r=(1-\Phi_f)/\tau_f$, [f] Not obtained

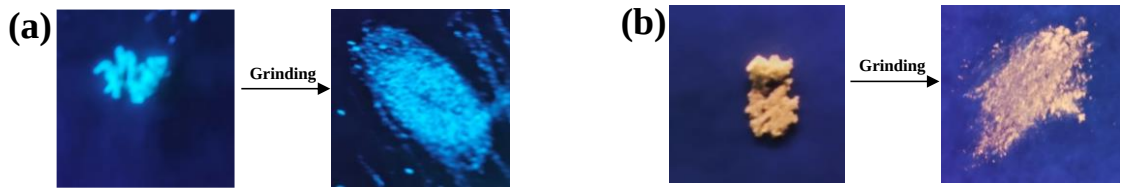

Figure S10. Photographs of (a) FA and (b) SOF at the initial, grinding and fumed under ultraviolet light

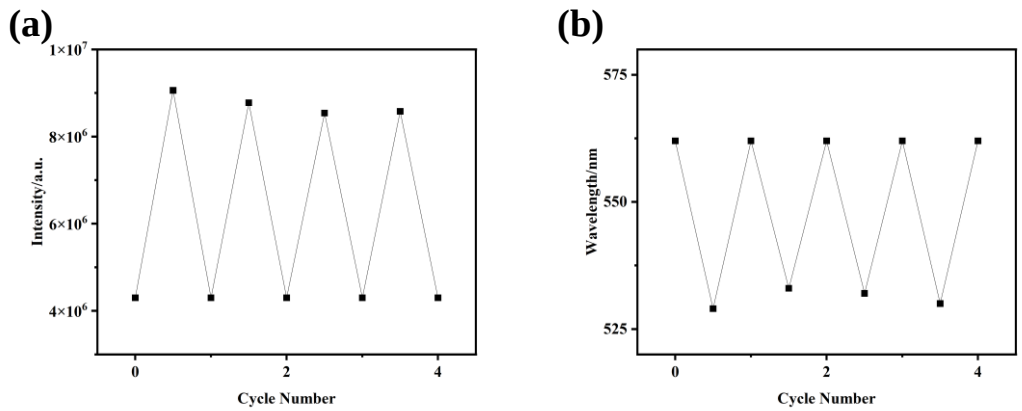

Figure S11. Reversible switching of the emission intensity and wavelength of DOF monitored. (The DOF first grinding then fumed with dichloromethane.)

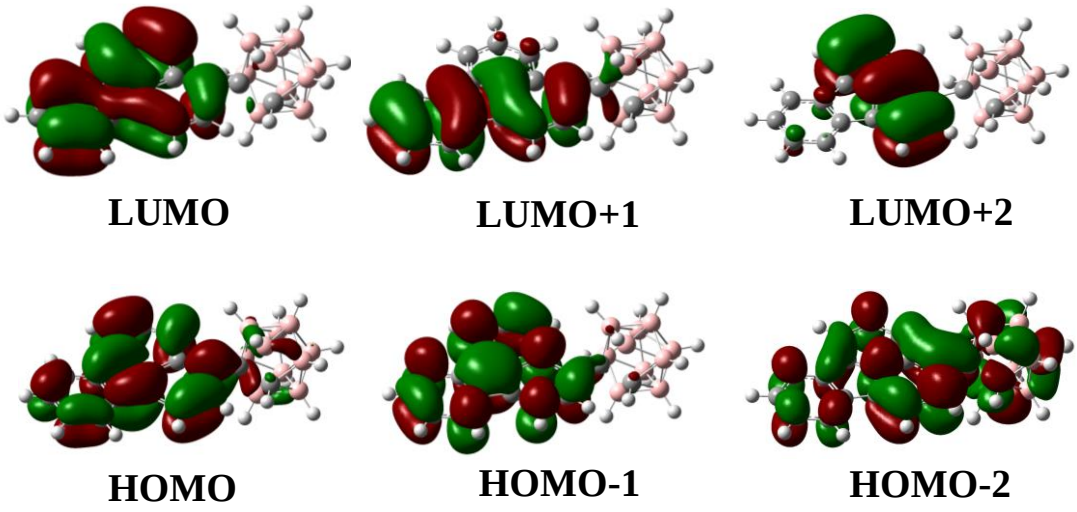

Figure S12. The theoretical calculated ground-state frontier orbitals contributions of SOF in gas sate using B3LYP/6-31G (d, p) level by Gaussian 09W.

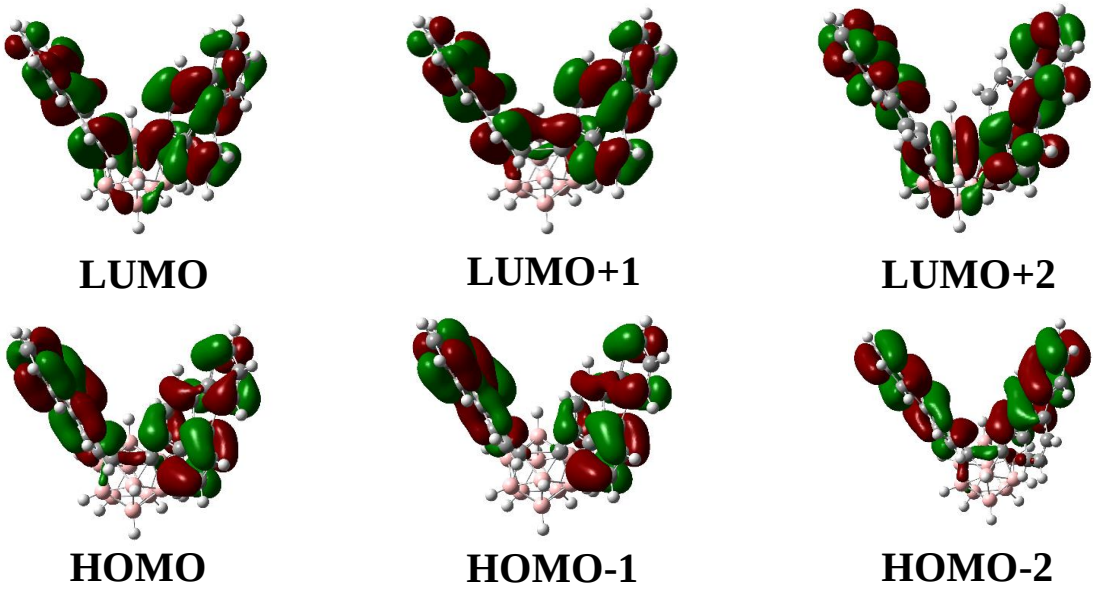

Figure S13. The theoretical calculated ground-state frontier orbitals contributions of DOF in gas sate using B3LYP/6-31G (d, p) level by Gaussian 09W.

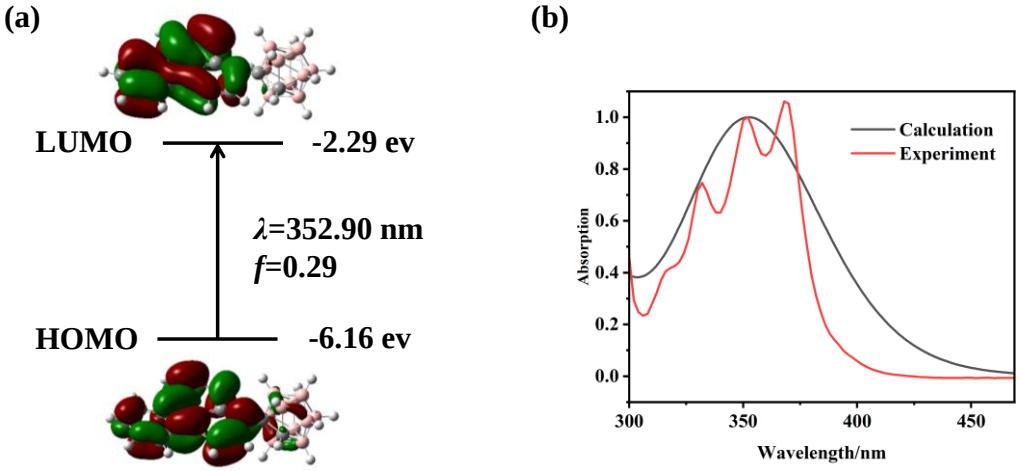

Figure S14. (a) The frontier molecular orbital transition diagram of the UV-visible absorption spectrum of compound SOF; (b) Comparison of theoretical and experimental UV-visible absorption spectra.

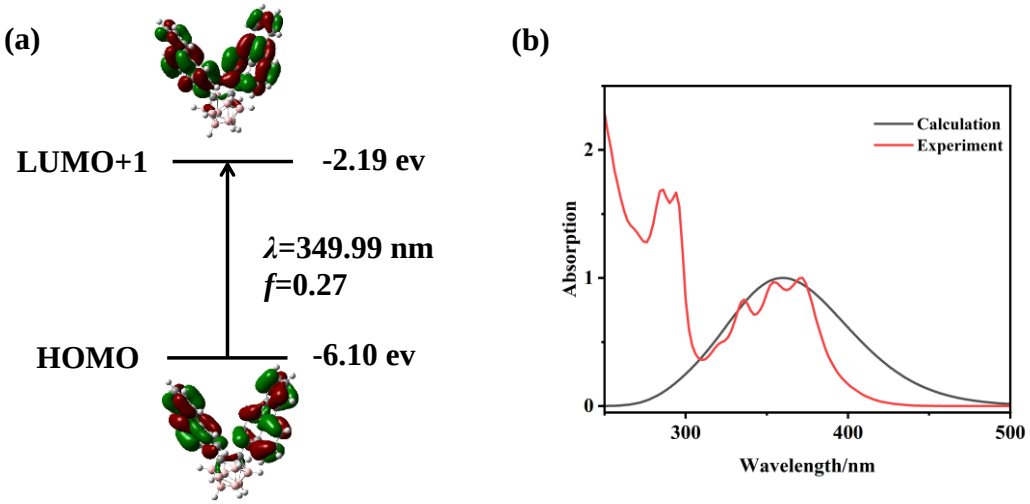

Figure S15. (a) The frontier molecular orbital transition diagram of the UV-visible absorption spectrum of compound DOF; (b) Comparison of theoretical and experimental UV-visible absorption spectra.

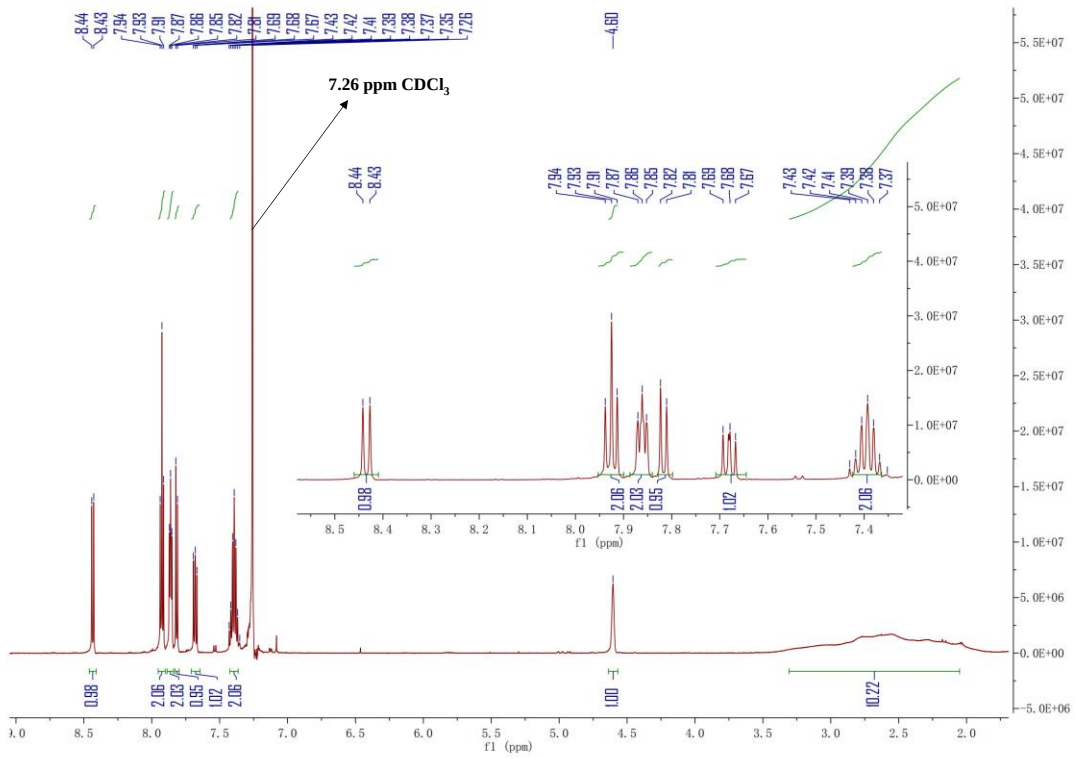

Figure S16. ^{1}H NMR spectroscopies of SOF in $CDCl_3$.

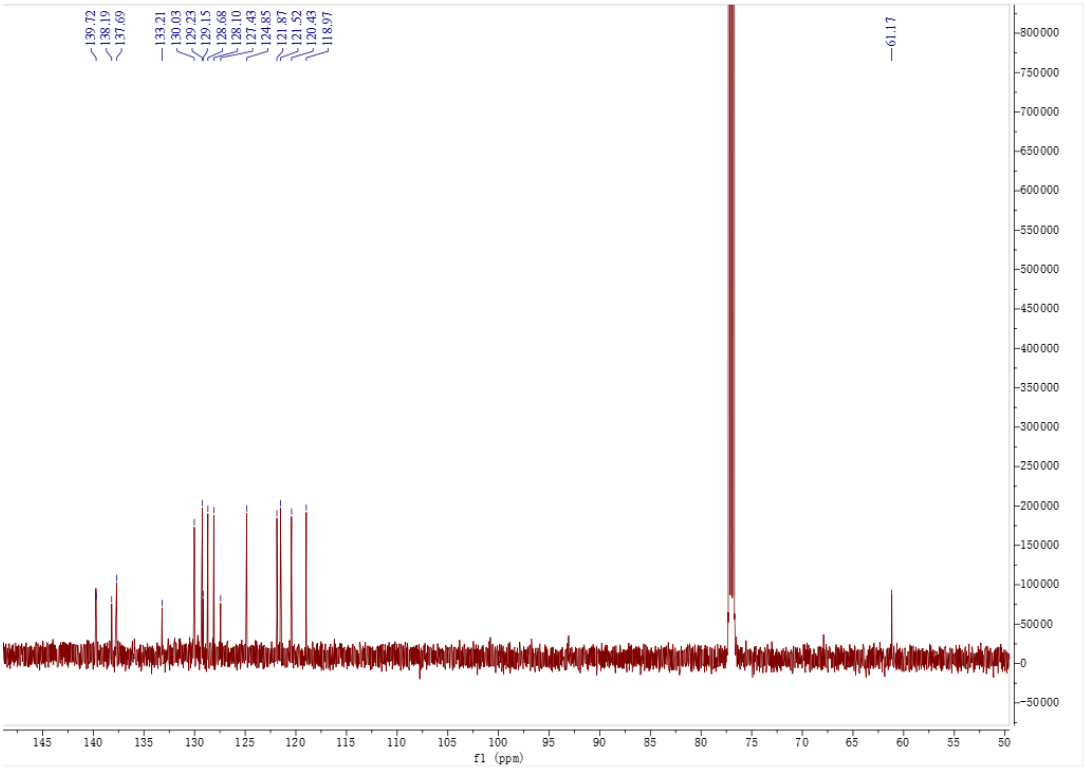

Figure S17. ^{13}C NMR spectroscopies of SOF in $CDCl_3$.

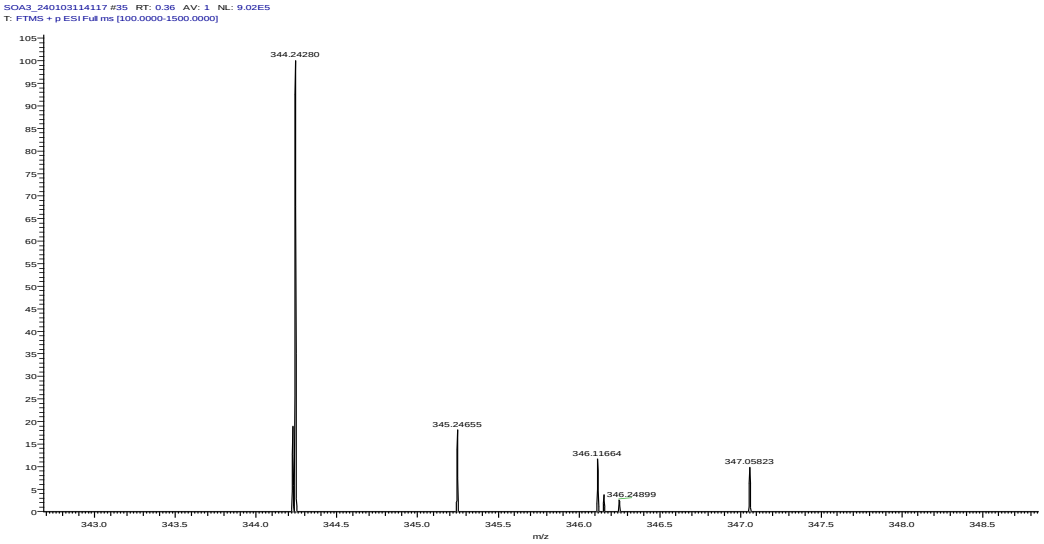

Figure S18. HRMS (ESI+) spectrum of SOF.

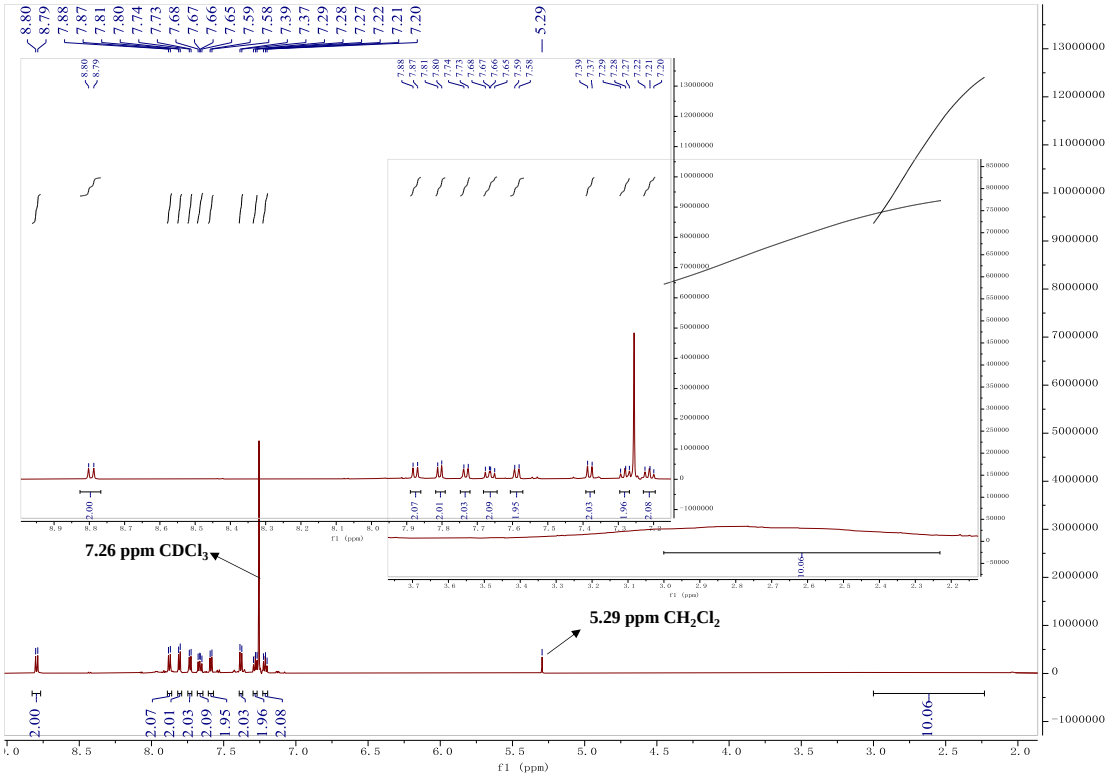

Figure S19. ^{1}H NMR spectroscopies of DOF in $CDCl_3$

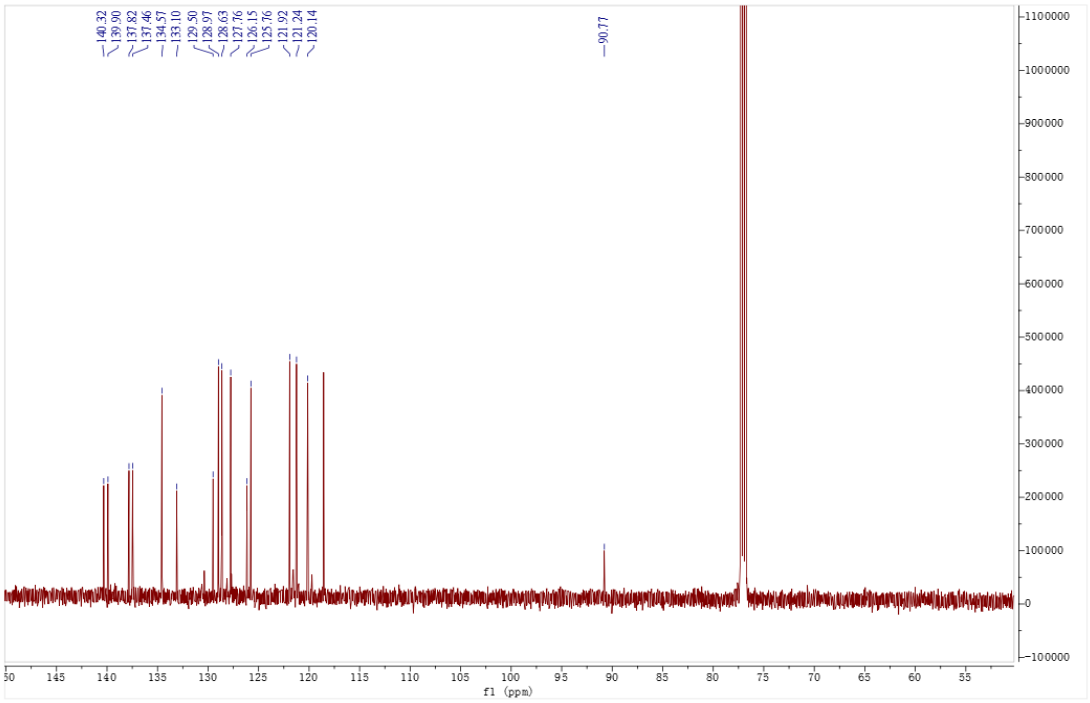

Figure S20. ^{13}C NMR spectroscopies of DOF in $CDCl_3$.

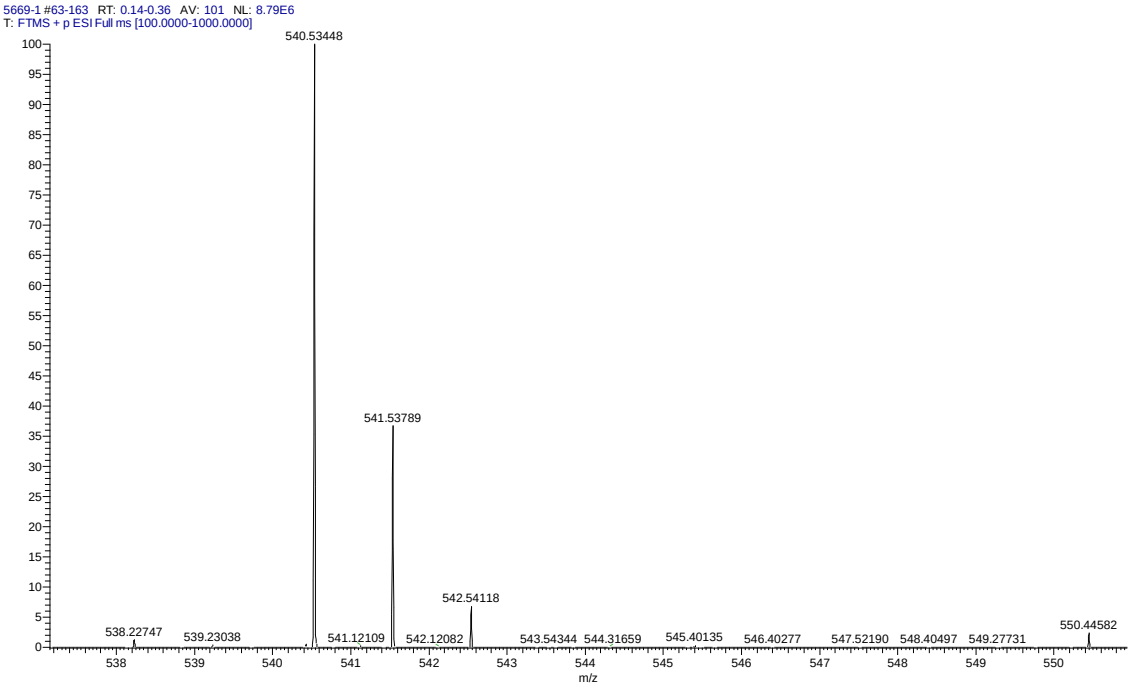

Figure S21. HRMS (ESI+) spectrum of DOF.